

## THE EFFECT OF IMMERSION TIME ON THE CORROSION BEHAVIOR OF SUS304 IN BRINE USING HALF-CELL POTENTIAL MEASUREMENT

Saber Rashid<sup>a</sup>, N. Islami<sup>a</sup>, A. K. Ariffin<sup>a\*</sup>, M. Ridha<sup>b</sup>, S. Fonna<sup>b</sup>

<sup>a</sup>Department of Mechanical and Materials Engineering  
Universiti Kebangsaan Malaysia, Bangi 43600, Selangor,  
Malaysia

<sup>b</sup>Department of Mechanical Engineering, Syiah Kuala University  
Jl. Tgk. Syech Abdul Rauf 7 Banda Aceh, Indonesia

### Article history

Received

18 December 2015

Received in revised form

10 March 2016

Accepted

25 April 2016

\*Corresponding author  
kamal3@ukm.edu.my

### Abstract

The aim of this study is to investigate the impact of immersion time, at different time values for two cases, with stressed and no stressed on materials. This study is conducted using SUS304 material with the presence of 3.5% NaCl at the range of stresses for the specimens lower than the yield strength. The geometry of the C-ring specimen was selected for 18.974 mm and 1.244 mm for the outer diameters and the thickness respectively. The immersion time effect was investigated using the half-cell potential measurement following the ASTM G-38 standard. The approach of corrosion environment was applied to resemble the condition of loading history. Three levels of stresses were designed and applied in finite element analysis and the results known as the parameters of stress-corrosion measurement. The ASTM G-38 standard is prominent for making C-ring stress-corrosion for elastic stress analysis. The stress-corrosion test was performed at two parameters, fixed stress and no stress. The value of stresses for fixed stress was chosen for 179.199 MPa, 328.665 MPa and 460.131 MPa, correspondingly. The immersion time were selected from 0, 10 and 30 days. The electrochemical result shows that the immersion time did not affect vastly to the corrosion behavior for no stress-corrosion compared with fixed stress. The corrosion rate increases proportionally with the time immersion increments due to the inability of the steel layer protection to regenerate itself. Subsequently, it is also due to the metal was exposed to plastic deformation that resulting the internal stresses due to the plastic anisotropy of the grains.

**Keywords:** stress corrosion; polarization curve; mechanical loading; Half-cell potential measurements

### Abstrak

Tujuan kajian ini adalah untuk mengkaji kesan masa rendaman, pada masa yang berbeza bagi dua kes, dengan daya pada bahan dan tiada daya pada bahan. Kajian ini dijalankan dengan menggunakan bahan SUS304 dengan kehadiran 3.5% NaCl pada julat daya yang dikenakan pada spesimen adalah lebih rendah daripada kekuatan luluh. Geometri spesimen cincin-C telah dipilih, iaitu 18.974 mm dan 1.244 mm masing-masing untuk diameter luar dan ketebalan spesimen. Kesan masa rendaman dikaji dengan menggunakan potensi ukuran separuh-sel mengikut standard ASTM G-38. Pendekatan persekitaran kakisan telah digunakan untuk menyerupai keadaan bebanan. Tiga tahap tekanan telah dipilih dan digunakan dalam analisis unsur terhingga. Hasil keputusan diketahui sebagai parameter pengukuran daya-kakisan. Standard ASTM G-38 penting untuk memilih daya-kakisan pada cincin-C untuk analisis tegasan elastik. Ujian tekanan kakisan telah dilakukan pada dua parameter, daya tetap dan tiada daya. Nilai daya tetap dipilih pada tiga nilai, iaitu 179.199 MPa, 328.665 MPa dan 460.131 MPa. Masa rendaman yang dipilih adalah 0, 10 dan 30 hari. Hasil elektrokimia menunjukkan bahawa masa rendaman tidak memberi kesan kepada tingkah laku kakisan tanpa daya berbanding dengan daya tetap. Kenaikan kadar kakisan berkadar dengan kenaikan masa rendaman kerana ketidakupayaan lapisan keluli untuk melindungi kesan kakisan. Juga, kakisan terhasil adalah disebabkan oleh logam itu terdedah kepada ubah bentuk plastik hasil daripada tekanan dalaman kesan daripada butiran anisotropy plastik.

**Kata kunci:** kakisan tekanan; keluk polarisasi; beban mekanikal; potensi ukuran separuh-sel

© 2016 Penerbit UTM Press. All rights reserved

## 1.0 INTRODUCTION

Stainless steels are widely used in manufacturing industries, due to their high strength and corrosion resistance in many environments. However, austenitic stainless steels are essentially iron, chromium, nickel consisting of sixteen to twenty five percent chromium and seven to twenty percent nickel. These alloys are referred to as austenitic since their structures remain solid solution (FCC,  $\gamma$  iron type) at all normal heat-treating temperatures. The presence of nickel, which is associated with FCC crystal structures, alters the FCC structure to be preserved at the heat-treating temperature. The high formability of the solid solution stainless steel is due to its FCC structure. Solid solution stainless steels ordinarily have higher corrosion resistance than ferritic and martensitic ones, since as a result of the carbides that are often preserved in the primary solid solution by the speedy cooling from hot temperatures, the chromium imparts a coating on the surface of a thin but extremely dense film of chromium oxide [1]. However, they have prominent problems such as pitting corrosion and stress corrosion cracking, which result with them, usually being replaced by SUS304 when used in aggressive environments [2].

The resistance of the stainless-steel is determined by its passive nature, alloy chemistry, heat treatment, precipitation morphology, kinetics and specific environment. The intactness of the passive film on the surface is dependent on its stability in the medium of exposure [3]. Even though the passive layer is an inexpensive means of corrosion protection, depending on the environment, it sometimes breaks down, causing severe localized corrosion attacks such as pitting, crevice and stress corrosion cracking, leading to catastrophic failures. Austenitic stainless steels (ASS) offer excellent corrosion resistance in many organic, acidic, industrial and marine environments. The non-magnetic properties, combined with exceptionally high toughness at all temperatures, make these steels an excellent selection for a wide variety of applications such as in chemical plants, and in the industrial and maritime fields [4]. Almost all metal components operate under mechanical loading and corrosive environments, and as such, stress caused by machining intactness and operation pressures is unavoidable. Many researchers have shown that stress plays an important role in the corrosion behavior of stainless steels [5-7].

Polarization mechanism is an important aspect in the corrosion analysis. Polarization measurements allowed determining the reaction at the corrosion potential are shown as polarization curves. The polarization measurement method allowed to determine the corrosion rate instantly based on electrochemistry concept [8]. These techniques may provide significant useful information regarding the corrosion mechanisms.

Based on mechanical of material, elastic stress that generated by mechanical loading in a material will have a significant influence for the polarization mechanism in the specific area. The internal stress that

also generated by mechanical loading will affected to the polarization mechanism. There is useful information for the researcher to analyse the corrosion behaviour of material during elastic stress occurred [8].

The above precipitates the investigation into the effects of different immersion times on the corrosion behaviour of the SUS304 in a 3.5 % NaCl medium. Therefore, the purpose of the present study is to clarify the effects of the immersion time on the corrosion behavior of type SUS304 at the range of lower than the yield, or what's known as the elastic stress applied.

## 2.0 EXPERIMENTAL PROCEDURES

### 2.1 Analytical and Computational Approach

Based on the standard of SCC specimen, the stress is calculated by reducing the thickness as it is expressed as follows [9]

$$ODf = OD - \Delta \quad (1)$$

$$\Delta = \frac{f\pi D^2}{4EtZ} \quad (2)$$

Where  $ODf$  is outside diameter after stressing,  $f$  is desired stress,  $\Delta$  is of deflection of OD giving by desired stress,  $D$  is mean diameter it equals to  $OD - \text{thickness}$ ,  $E$  is modulus of elasticity, and  $Z$  is a correction factor for curved beams as in figure 1. Since the deflection is a parameter as an input data, using equation (2), the scale of deflection which used to obtain the stress in the specimen were calculated by:

$$f = \frac{\Delta 4EiZ}{\pi D^2} \quad (3)$$

The C-ring sample, as generally used is a constant-strain specimen. Tensile stress produced on the exterior of the ring by tightening a bolt centered on the outside diameter (OD). The level of stress described by adjusting the outside diameter of samples. To predict the desired stress, the compression tests were conducted to the C-ring sample. Figure 2 shows the relation of OD deflection and load. By using compression test result, three levels of load have been applied for corrosion measurement.

Compression test was carried out to obtain the yield point of the specimen. Based on compression test result, three levels of deflection are specified to the samples. Finite element approaching is conducted to estimate the desired stress during loading by the deflection. Results of estimated stress are used to obtain the relation of corrosion behaviour and stress during applied load. A commercial finite element analysis Abaqus<sup>LM</sup> 61.6 was implemented for this study, the finite element module analysis the following, the dimension and material properties of the actual sample. This approach is to obtain the relevance of polarization curve and each level of stress.

Figure 4 (a) and (b) shows that the maximum of elastic point for the c-ring sample is at a 0.0 mm and 0.7 mm deflection. This number is applied as the maximum

load for the C-ring sample. Therefore, one level of deflection was selected to investigate the effects of immersion on the polarization curve.

Table 3 shows the relationship between the deflection of OD, applied load for the C-ring and the estimated stress on the exposed area. All data for  $D$ ,  $\Delta D$ ,  $d$  and  $t$  are in millimeters.  $E$  is the modulus of elasticity of the

material (MPa),  $Z$  is a correction factor for curved sample which depends on the  $D/t$  ratio. In the case of the present C-ring specimens amounts of  $Z=0.94$ , as shown in Figure 1, available at [9]. The relationship between the change in the inner and the outer diameter shows the stress as shown in the Table 3.

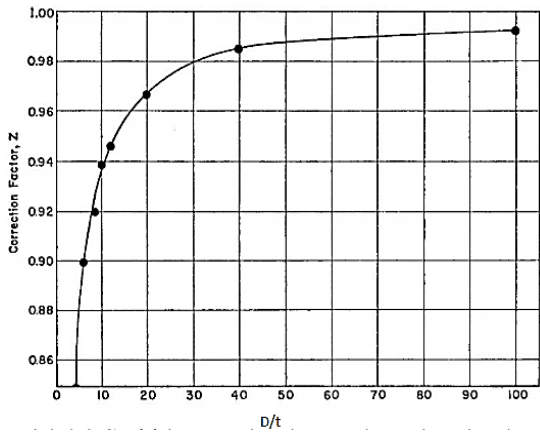


Figure 1 Corrosion factor for curve from ASTM-G38 Standard.

2.2 Prediction of Desired Stress

Estimation of desired stress on the surface of C-ring specimen by using finite-element analysis is necessary, to recover the utilization of a strain gauge following the reference ASTM G-38. Visualization of stress using finite-element analysis improved efficiency and clearly partitioned the gradient of stress levels on the surface of C-ring specimen.

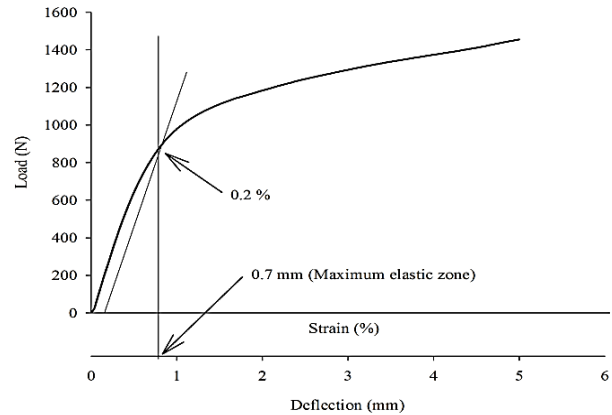


Figure 2 The relation of OD deflection and load resulted by compression test

Therefore the exposed area for the polarization measurement obtainable in the respected area. The model for finite element analysis using similar shape of the polarization experimental specimen Figure 4. Others parameter such as dimension, material properties and deflection of applied load absolutely same to the prepared specimens. Table 1 shows the relationship between the deflection of OD, applied load for the C-ring and the estimated stress on the exposed area.

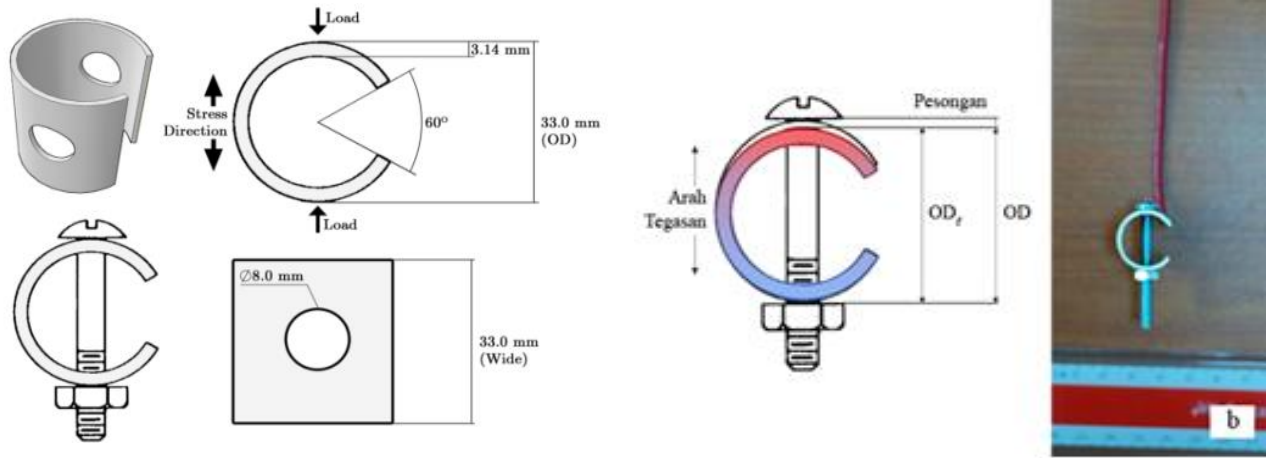
Table 1 Deflection by Loading

Type	OD Deflection (mm)	Load (N)	Maximum Stress at exposure area (MPa)
Load 1	0.3002	402.999	197.199
Load 2	0.5003	640.226	328.665
Load 3	0.7001	819.021	460.131

2.3 Materials and Specimen

The samples were cut from SUS304 tube. The chemical composition of the material (wt. %) is listed in Table 2. The specimen surface was mechanically polished with P120, P600 and P2000 grit papers and then followed by

washing with distilled water. The specimens were formed into c-ring shapes according to the ASTM G-38 Standard as shown in Figure 3 (a) and (b). It was important to assure that the stuff being used was SUS304 and the modulus of elasticity ( $E$ ) was fixed for each type of fabric as pictured in Table 3.



(a) Size and shape of the specimen used based on ASTM G38 standard

(b) Illustrates the loading mechanism and the actual image of the specimen used.

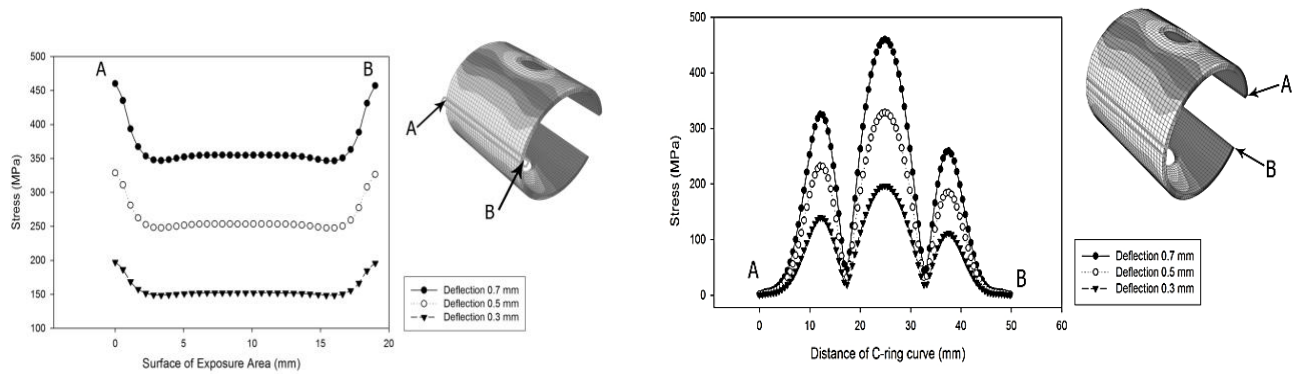
Figure 3 Specimen used based on ASTM G-38 standard

Table 2 The nominal composition of SUS304 (wt. %)

Element	%C	%Si	%Mn	%P	%S	%Cr	%Ni	%Mo
	0.75	0.36	0.26	0.018	0.010	3.30	0.12	4.50

Table 3 Relationship between stress and deflection

Specimens	Modulus of Elasticity, E (GPa)
I	220
II	214
III	193



(a) Stress distribution at perpendicular to the deflection.

(b) Stress distribution at the edge of the sample.

Figure 4 Stress distribution on the surface area of C-ring shape.

## 2.4 Method of Electrochemical Measurements.

To keep the effects of polarization and in turn, to be able to estimate the grade of corrosion that occurred with the specimens, it was necessary to build up a set of electrochemical measurement equipment. The ASTM G-108 was used as a reference for obtaining the answers. The ASTM G-108 standard describes the steps that must be carried in order to carry on the electrochemical measurement of the SUS 304 stainless steel specimens.

The electrochemical measurements were done using samples with 10x10 mm working area. The trials were also taken at 3.5 % NaCl solution at room temperature. The working electrode (WE) was the sample material and the reference electrode was Ag/AgCl (Silver Chloride Electrode). The specific configuration parameters for these measurements are presented in Table 4.

**Table 4** Potentiodynamic scan configuration

Software	LAB View and IVMAN 1.1 Electrochemical Workstation
Hardware	ZIVE PP1 (Korea)
Filter	60Hz
Type of Scan	Potentiodynamic
Reference Electrode	SSE (Silver Chloride Electrode)
Step Increment	1 mV
Scan Rate	0.6 mV/s
Current Range	Auto
Current Interrupt	Auto
Area of Specimen	10x10 mm

## 2.5 Immersion Method

Three immersion times were used to assess the changes in the polarization. For this goal, the ASTM G44 standard was used as a guide in making artificial seawater. 3.5 % NaCl (Sodium Chloride) was added to the required quantity of distilled water. Figure 5 (a) and (b) shows the exposed area on the specimen and the concentration of the specimens in the 3.5% NaCl solution.

Furthermore, to obtain an appropriate field of vulnerability on the specimen, a protective coating process was carried out using Isolators. The exposed part of the specimen was only opened as wide as 10 mm<sup>2</sup> in the area estimated to receive the highest levels of stress. The final stage of the specially made salt bridge was aimed straight at the exposed area on the specimen. Figure 5 shows the exposed area on the specimen and the immersion of the specimens into the 3.5% NaCl solution.

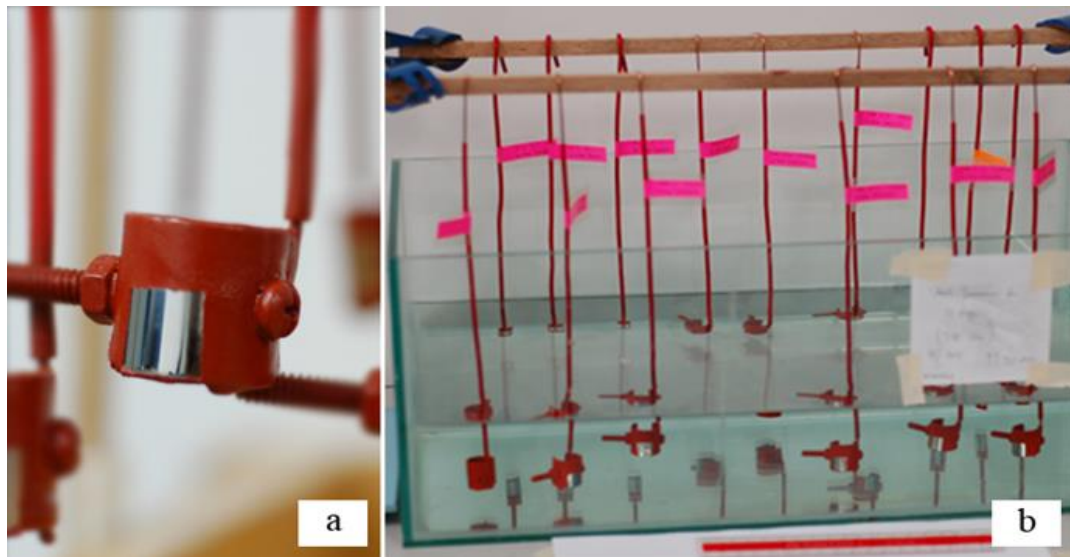


**Figure 5** (a) Specimen with 1 cm<sup>2</sup> area of exposure, and (b) Immersion of specimens in container

The specimens were immersed in the specified period of time. The longest point of concentration was necessary in order to watch the result of the immersion following the strain imposed on the specimens.

In this manner, the result of the immersion could be worked into one of the parameters of measurement in this study into the relationship between immersion and the nature of erosion. The prepared specimens were soaked for 0 hours, 240hours and 720 hours. Table 5 outlines the immersion scheme and the stress on the specimens.

**Table 5** Immersion of specimens into a solution of 3.5% NaCl

	Normal	Deflection 0.3 mm (197.19MPa)	Deflection 0.7 mm (460.13 MPa)
Without immersion	3 Specimens	1Specimens	3 Specimens
Immersion 240 hours	3 Specimens	1Specimens	3 Specimens
Immersion 720 hours	3 Specimens	1 Specimens	3 Specimens

### 3.0 RESULTS AND DISCUSSION

#### 3.1 Assessment of the Specimen Subjected to No Stress

##### 3.1.1 Polarization Of The Specimen Subjected To No Stress And No Immersion.

As an initial step three polarization curves generated for a specimen at zero stress is proven in the Figure 6. Because the anodic and cathodic potential-current density relationship are not quite symmetric, the condition known as faradaic rectification is presented. [10] The corrosion potential versus current density for the SUS304 at zero stress without immersion in NaCl solution has been taken as an initial step, with three polarization curves generated showing a similar trend. The corrosion potential was shown at -533.503mV and the current density in these conditions were 6.161  $\mu$ A. Anode polarization curves under these conditions showed the region of passivation, which indicate that the passive layer on the surface of the stainless steel was damaged, as can be seen from the grave in Figure 6 and Table6

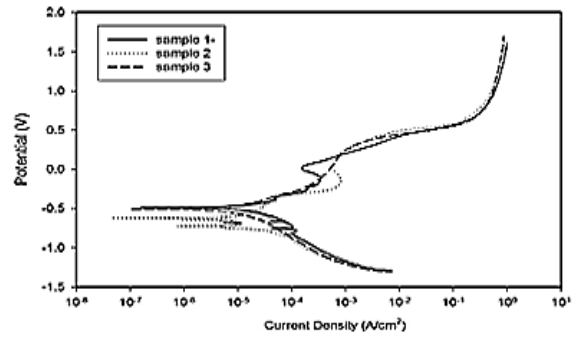


**Figure 6** Polarization curve at zero stress, no immersion

**Table 6** Polarization curve data for zero stress with no immersion

Sample	E <sub>corr</sub> (mV)	I <sub>corr</sub> ( $\mu$ A)	R <sub>p</sub> (K $\Omega$ )	CR (mpy)
1	-533.503	6.161	8.792	2.492
2	-667.224	6.183	9.610	2.501
3	-512.535	3.983	6.181	1.611

##### 3.1.2 Polarization Of The Specimen Subjected to No Stress And 10 Day Immersion.

The materials without stress, immersion time did not show a significant influence for the behaviour of polarization corrosion. Figure 7 of the three polarization curves generated showing the polarization curve of no stress with 3.5% NaCl solution for no immersion. These curves indicate a similar style. Corrosion potential was shown at -494mV and the current density in these conditions was 2.87  $\mu$ A, as depicted in Figure 7 and Table7. The corrosion potential was demonstrated at -494 MV and the current density in these conditions was 2.87  $\mu$ A. Anode polarization curves under these conditions showed the region of passivation, which indicate that the passive layer on the surface of the stainless steel was damaged, as can be seen from the grave in Figure7

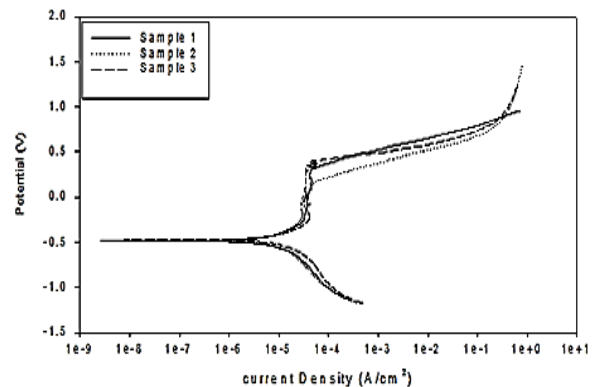


**Figure 7** Polarization of the specimen subjected to no stress and 10 day immersion

**Table 7** Polarization of the specimen subjected to no stress and 10 days immersion

Sample	E <sub>corr</sub> (-mV)	I <sub>corr</sub> (μA)	R <sub>p</sub> (KΩ)	CR (mpy)
1	-494	2.87	9.998	3.292
2	-488	5.679	8.833	2.297
3	-468	8.139	5.596	1.611

**3.1.3 Polarization Of The Specimen Subjected To No Stress And 30 Day Immersion.**

Three polarization curves show a similar trend as shown in figure 8. Corrosion potential was shown at -488mV and the current density in these conditions was 4.512 μA.

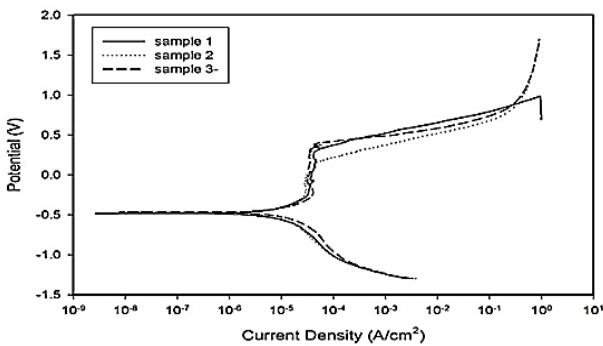


**Figure 8** Polarization curve at 460.131 MPa stress for 10 days Immersion

**Table 8** Polarization curve data for 460.131 MPa stress with 10 days immersion

Sample	E <sub>corr</sub> (-mV)	I <sub>corr</sub> (μA)	R <sub>p</sub> (kΩ)	CR (mpy)
1	-488	4.512	8	21.279
2	-480	5.674	3.276	14.853
3	-468	6.232	2.396	20.309

The polarization of the specimen subjected to no stress, the materials without stress, immersion time did not show a significant influence for the behaviour of polarization corrosion.

**3.2 Assessment of the Specimen Subjected to 460.131 MPa Stress**

**3.2.1 Polarization Of The Specimen Subjected To 460.131 Mpa Stress With 3.5% NaCl Solution For No Immersion**

Figure 9 of the three polarization curves generated showing the polarization curve of 460.131 MPa stress with 3.5% NaCl solution for no immersion. These curves show a similar trend. Corrosion potential was shown at -913.376mV and the current density in these conditions was 52.615μA, as shown in Figure 9 and Table9.

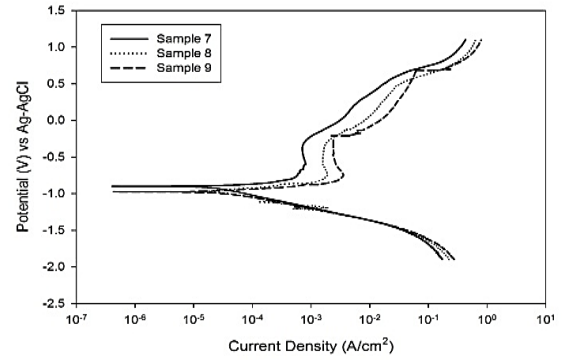


**Figure 9** Polarization curve at 460.131 MPa stress with no immersion

**Table9** Polarization curve data for 460.131 MPa stress with no immersion

Sample	E <sub>corr</sub> (-mV)	I <sub>corr</sub> (μA)	R <sub>p</sub> (kΩ)	CR (mpy)
1	-913.376	52.615	1.307	21.279
2	-987.244	36.893	3.276	14.853
3	-996.246	50.216	2.396	20.309

**3.2.2 Polarization of the specimen subjected to 460.131 MPa stress with 3.5% NaCl solution for 10 days immersion**

The three polarization curves show a similar trend. Corrosion potential was shown at -805.115mV and the current density in these conditions was 191.905μA, as shown in Figure 10 and table 10.

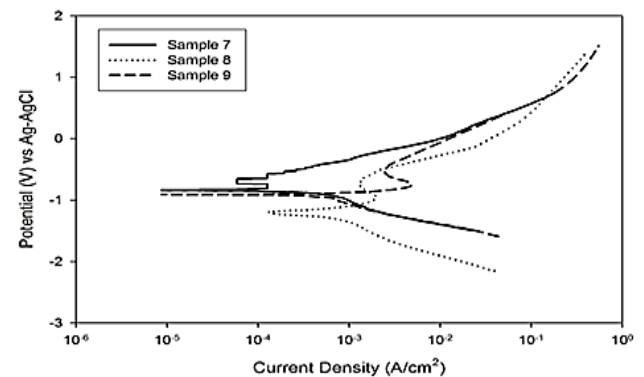


**Figure10** Polarization curve at 460.131 MPa stress for 10 days immersion

**Table10** Polarization curve data for 460.131 MPa stress with 10 days immersion

Sample	E <sub>corr</sub> (mV)	I <sub>corr</sub> (μA)	R <sub>p</sub> (KΩ)	CR (mpy)
1	-805.115	191.905	626.0	77.613
2	-1,262	187.851	640.851	75.922
3	964.923	181.767	660.829	73.512

**3.2.3 Polarization Of The Specimen Subjected To 460.131 Mpa Stress With 3.5% Nacl Solution For 30 Days Immersion**

In Figure 11 and table 11, the three polarization curves show a similar trend. Corrosion potential was shown at -889.958mV and the current density in these conditions were 232.615µA.

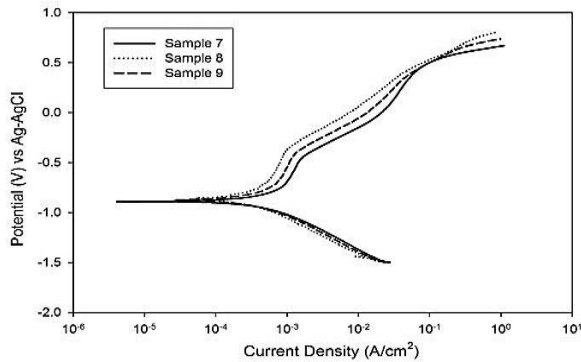


**Figure 11** Polarization curve at 460.131 MPa stress for 30 days immersion

**Table 11** Polarization curve data for 460.131 MPa stress with 30 days immersion

Sample	Ecorr (mV)	Icorr (µA)	Rp (KΩ)	CR (mpy)
1	-889.958	232.615	133.683	94.100
2	-846.252	241.023	90.077	97.478
3	-867.929	251.880	100.641	87.246

**3.3 Assessment of the Effect of Immersion Time for Specimen Subjected to 179.199 MPa Stress.**

Figure 12 and table 12 shows the polarization curve of three levels of immersion. This curve shows the significant difference in the number of Icorr, which the difference of Icorr has greatly affected to the corrosion rate of the material. The curve also shows the number of Ecorr not strongly different. It is measured at -518.948 mV. Ecorr number is strongly different when compared to Ecorr on a sample with 30 days immersion, with the number of Ecorr at 841.112 mV. Therefore, can understand the behaviour of material under mechanical loads was more anodic while immersed in the 3.5% NaCl solution [8]. This curve also shows the number of Icorr significantly different according to the level of immersion time. The difference of Icorr number is strongly affected to the corrosion behaviour of each sample.

This information useful for investigating the relation between immersion and the corrosion behaviour of materials.

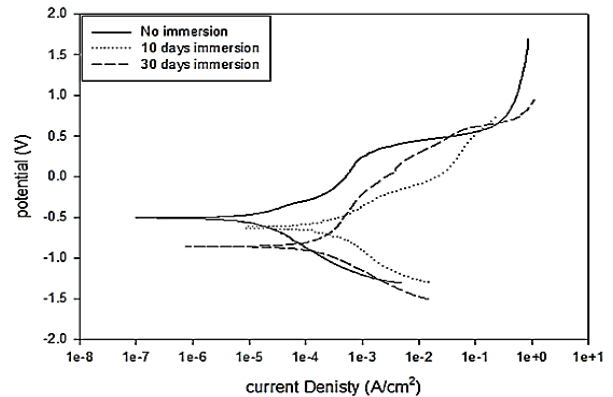


**Figure 12** Polarization curve of 3 levels of immersion for 179.199 MPa

**Table 12** The Polarization curve data for three levels of immersion time for 179.199 MPa.

Immersion time	Ecorr (mV)	Icorr (µA)	Rp (KΩ)	CR (mpy)
0 day	-518.9	10.1	5.6	2.0
10 days	-584.6	56.6	1.0	11.4
30 days	-841.1	103.8	884.4	20.9

Based on the past polarization curves, the three levels of immersion time, which have highest corrosion behavior on the 30 day immersion. Figure 13 shows the highest number of CR (mpy) 20.935 at a level of 30 day immersion as showed in Figure 13.

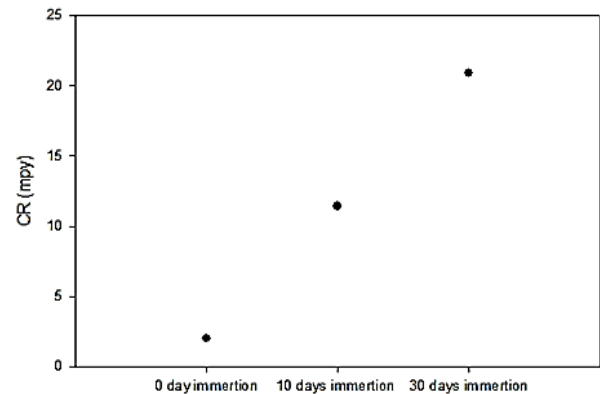


**Figure 13** The Relationship of immersion and CR.

### 3.4 Relationship Between Immersion Time and CR for Stressed and Non-Stressed Material.

In Figure 10, immersion time has been compared with the maximum CR for both the stressed and non-stressed, each immersion time in order to look at the relationship between the immersion time and the effects of polarization, by using the same level of stress, on all C-rings. Polarization can be interpreted based on the CR, which is calculated using the extrapolation of the gradient Tafel graph the aim is to look at the relation between the immersion effects of polarization, Immersion time is not strongly affected to the corrosion behaviour for non-stressed material compared to stressed material, belong to the changes in polarization curve, as shown in Figure 10.

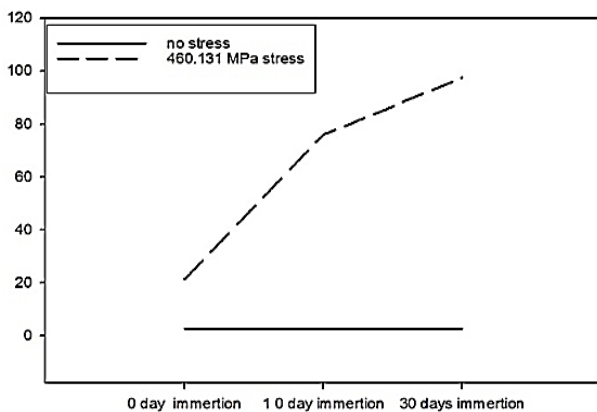


Figure 14 Relation of Stress and Corrosion rate.

## 4.0 CONCLUSION

The effect of immersion time on the corrosion behaviour of SUS304 in brinewas investigated, the result concluded as the followings:

- the immersion time is not strongly affected to the corrosion behavior for no stressed material compared to stress material.
- The relationship between the immersion time and CR has shown the immersion time is an essential factor to increase the corrosion behavior of SUS304 during applied load.

- The stress calculation in ASTM G-38 was not clearly show the relevant number of the properties of austenitic SUS304.
- Finite-element analysis is use to improved the efficiency and clearly partitioned the gradient of stress levels and the location of maximum stress on the surface of C-ring specimen.

## Acknowledgement

The author would like to acknowledge the University Kebangsaan Malaysia (UKM), especially in the laboratory of ZWICK for allowing the research to be conducted the experimental.

## References

- [1] Gebрил, M.A., Aldlemey, M.S., Haider, F.I. and Ali, N. 2014. Effect of Austenizing and Tempering Time on Corrosion Rate of Austenitic Stainless Steel in Oxalic Acid. *Advanced Materials Research*. 980: 46-51.
- [2] Moura V.S., Lima, L.D., Pardal, J.M., Kina, A.Y., Corte, R.R.A. and Taveras, S.S.M. 2008. Influence Of Microstructure On The Corrosion Resistance Of The Duplex Stainless Steel UNS S31803. *Materials Characterization*. 59(8): 1127-1132.
- [3] Aydogdu, G. and M. Aydinol. 2006. Determination Of Susceptibility To Intergranular Corrosion And Electrochemical Reactivation Behaviour of AISI 316L Type Stainless Steel. *Corrosion Science*. 48 (11): 3565-3583
- [4] Tsay, L., Yu, S.C., Chyou, S-D. and Lin, D-Y. 2007. A Comparison Of Hydrogen Embrittlement Susceptibility Of Two Austenitic Stainless Steel Welds. *Corrosion Science*. 49(10): 4028-4039.
- [5] Paredes, E.C., Bautista, A., Alvarez S.M. and Velasco, F. 2012. Influence Of The Forming Process Of Corrugated Stainless Steels On Their Corrosion Behaviour In Simulated Pore Solutions. *Corrosion Science*. 58: 52-61.
- [6] Contreras, A., Hernandez, S.L., Orozco-Cruz, R. and Galvan-Martinez, R. 2012. Mechanical And Environmental Effects On Stress Corrosion Cracking Of Low Carbon Pipeline Steel In A Soil Solution. *Materials & Design*. 35: 281-289.
- [7] Du, X.S., Su, Y.J., Li, X.J., Qiao, L.J. and Chu, W.Y. 2012. Stress Corrosion Cracking Of A537 Steel In Simulated Marine Environments. *Corrosion Resistance*. 65: 278-287.
- [8] Badea, G.E., Caraban, A., Sebesan, M., Dzitac, S., Cret, P. and Setel, A. 2010. Polarisation Measurement Used For Corrosion Rates Determination. *Journal of Sustainable Energy*. 1(1): 1-4.
- [9] ASTM, ASTM: 38. 2001. *ASTM International Publisher*, West Conshohocken, PA
- [10] Butler, B. M., Chopra, M. B., Kassab, A. J. and Chaitanya, V. 2013. Boundary Element Model For Electrochemical Dissolution Under Externally Applied Low Level Stress. *Engineering Analysis with Boundary Elements*. 37(6): 977-987.